Absorption Cross-Section Measurements of a Human Model in a Reverberation Chamber

Damir Senic, *Member, IEEE*, Antonio Šarolić, *Member, IEEE*, Zbigniew M. Jóskiewicz, and Christopher L. Holloway, *Fellow, IEEE*

Abstract—We provide the results of human body absorption cross-section (ACS) measurements. The setup was based on the reverberation chamber as a well-known measurement environment capable of performing ACS measurements. The approach was supported by reference measurements on canonically shaped objects which were convenient for analytical (Mie scattering theory) ACS calculations. Measured ACS of canonical objects was in excellent agreement with calculated values. The ACS measurements of a human model were performed: 1) on an actual human body in an upright posture and 2) on a cylindrical water model made of vertically stacked water-filled jugs. The cylindrical model had the same water content as an average human body. Comparison between these two models showed a small difference in measured ACS within the measurement uncertainty of our setup. Thus, the cylindrical water model proved to be a useful artifact, especially for time-consuming broadband ACS measurements.

Index Terms—Absorption cross-section, absorption effectiveness (AE), human exposure, loading, *Q*-factor, reverberation chamber.

I. INTRODUCTION

MODERN communications take place in various and generally complex electromagnetic environments. Sources of electromagnetic radiation, whether intentional or unintentional, are present in any environment including living and working spaces as well as aircraft and automobiles. The electromagnetic field distribution in such environments is highly nonuniform and strongly depends on characteristics of the environment in which communication takes place. Multiple reflections, transmissions, and diffractions, which are characteristic of such environments, arise as a consequence of the environment's electrical properties and the presence of the lossy objects.

If the observed environment is highly reflective, then its quality factor Q, defined as the ratio of the stored energy and dissipated power inside the environment [1], represents an essential indicator of the environment's electromagnetic behavior.

Besides communication aspects, the environment Q determines human exposure to electromagnetic fields. Relevant standards for assessing human exposure exhibit a deficiency regarding closed reverberant (diffuse) environments. In fact, the available literature regarding human exposure presumes plane-wave exposure in the free space, which generally does not well represent many real exposure situations.

Propagation characteristics inside environments populated by lossy objects that influence the Q factor are commonly studied for different means of transportation [2]–[4]. In such environments, viewed as resonators with an internal modal structure, the presence of RF sources can lead to the forming of "hot-spots" where the electromagnetic field has a significant level. However, in a real situation, apertures, such as windows and doors, and absorbing objects, such as passengers and seats, absorb part of the energy accumulated inside the observed environment and lower its Q factor.

The presence of different lossy objects inside the reverberant environment changes its Q and affects the electromagnetic field amplitude as well as locations of maximum and minimum field levels. The absorption cross-section (ACS) presents a very important parameter of any lossy object placed within a highly reflective environment, and excited by an RF field. Due to the large number of incident plane waves, the ACS is generally given as an average over different incidence angles and polarizations.

In this paper, we present a study of the power dissipated (in terms of the ACS) within an average human body in an upright posture inside a mode-tuned reverberation chamber. Before performing the measurements on a real human body, the approach was verified on lossy spherical objects whose ACS could be determined analytically. Only the verification measurements were performed at NIST; no human tests were performed at NIST or by NIST personnel. Human-body measurements included 1) a real human body and 2) a cylindrical water model made of vertically stacked water-filled jugs.

The outline of the paper is as follows. In Section II, the motivation for analyzing the human body ACS is discussed and the theoretical background of the ACS is reviewed. Section III illustrates the proposed measurement setups and techniques used for determining the ACS. Section IV summarizes the results and findings. In Section V, we follow with the validation of the measurement setup and measurement uncertainty. Final conclusions are given in Section VI.

II. ACS—THEORETICAL BACKGROUND

The ACS measurements of lossy objects within a reverberation chamber were performed in [5]. The method is based on measuring the average power transmission between two antennas with and without the lossy object present in the chamber [6].

The ACS represents the lossy object's surface area that absorbs the incident electromagnetic power. It is generally smaller than the actual lossy object's surface area due to the fact that a portion of the power incident on the exposed lossy object can be reflected from or transmitted through the lossy object. The ACS depends on the frequency, incident wave direction, and polarization. It is defined as the ratio of the power absorbed by the exposed lossy object P_{abs} and power density incident on the exposed lossy object S_{inc}

$$\text{ACS} = \frac{P_{\text{abs}}}{S_{\text{inc}}}. \tag{1}$$

The absorbed power can be expressed in terms of the exposed lossy object's mass m and whole-body specific absorption rate (WBSAR), which represents a measure of the exposure due to the electromagnetic fields [7], Thus, ACS can be written as

$$\text{ACS} = \frac{\text{WBSAR} \cdot m}{S_{\text{inc}}}. \tag{2}$$

According to (2), we can determine the WBSAR by knowing the power density incident on the exposed object, its mass, and associated ACS. Therefore, the knowledge regarding the behavior of the ACS for various human models and postures is of utmost importance for developing a useful model for assessing human exposure to the electromagnetic fields inside highly reflective (diffuse) environments. Recent studies of human exposure to the electromagnetic fields in diffuse environments can be found in [8]–[13]. The ACS of a human body in various postures was studied in [2], [14]–[17]. In this paper, we present the broadband ACS results of a human body in an upright posture measured inside a mode-tuned reverberation chamber.

The measurement approach is based on a power balance theory [18], wherein the resonant cavity total Q can be expressed as a combination of four different contributions

$$Q^{-1} = Q_1^{-1} + Q_2^{-1} + Q_3^{-1} + Q_4^{-1} \tag{3}$$

where Q_1 is related to the losses in imperfect metallic walls, Q_2 is related to the losses due to the absorption in lossy objects, Q_3 is associated with the losses due to the apertures, and Q_4 is related to the losses in the measurement antennas. The second term on the right-hand side in (3) is inversely proportional to the ACS

$$ACS = \frac{2 \cdot \pi \cdot V}{\lambda} \cdot Q_2^{-1} \tag{4}$$

where V is the cavity volume and λ is the wavelength. Adding a lossy object to a reverberation chamber (loaded cavity) changes the Q as follows $Q_{\text{loaded}}^{-1} = Q_{\text{unloaded}}^{-1} + Q_2^{-1}$. Hence, by measuring the loaded and unloaded cavity Q, we can determine lossy object's ACS as

$$\langle ACS \rangle = \frac{2 \cdot \pi \cdot V}{\lambda} \cdot \left(Q_{\text{loaded}}^{-1} - Q_{\text{unloaded}}^{-1} \right) \tag{5}$$

where the brackets denote an ensemble average over paddle orientations.

Generally, measurements in a reverberation chamber are simplified by measuring the scattering S parameters. To determine the ACS of an object placed inside a reverberation chamber, it is necessary to measure the forward transmission coefficient S_{21}, whose squared value is equal to the ratio of received and transmitted power. The theory given above assumes lossless and perfectly matched antennas. Since antennas, generally, cannot be assumed perfectly matched, the normalized transmission factor G, instead of S_{21} is used [18]

$$G = \frac{\left\langle |S_{21}^s|^2 \right\rangle}{\left(1 - |\langle S_{11} \rangle|^2 \right) \cdot \left(1 - |\langle S_{22} \rangle|^2 \right)} \tag{6}$$

where $|S_{21}^s|$ is the magnitude of the stirred component of the forward transmission coefficient, and S_{11} and S_{22} are measured reflection coefficients of transmit and receive antennas, respectively. The ACS can then be easily calculated from known G factors for the chamber loaded with the absorbing object G_{loaded} and the unloaded chamber G_{unloaded}

$$\langle \text{ACS} \rangle = \frac{\lambda^2}{8 \cdot \pi} \cdot \left(\frac{1}{G_{\text{loaded}}} - \frac{1}{G_{\text{unloaded}}} \right)$$
$$= \frac{\lambda^2}{8 \cdot \pi} \cdot \frac{G_r - 1}{G_{\text{unloaded}}} \tag{7}$$

where relative normalized transmission is $G_r = G_{\text{unloaded}}/G_{\text{loaded}}$.

III. MEASUREMENT SETUPS AND TECHNIQUES

Reverberation chambers were used to determine the human body ACS. In order to verify the validity of the approach, prior to measuring the ACS of the human body, we measured the ACS of spheres that could be determined analytically using the Mie series method [19]. Therefore, two different setups were prepared, one for the reference measurements and another for the human-body measurements.

A. Reference Measurements

All reference measurements were performed inside an aluminum reverberation chamber with dimensions: (L) 1.49 m × (W) 1.16 m × (H) 1.45 m. According to [20] and [21], this size of the reverberation chamber enables measurements starting from approximately 1 GHz. The reverberation chamber was equipped with a single aluminum mechanical stirrer mounted between ceiling and floor. The stirrer rotated about a vertical axis within a cylindrical volume 1.1 m in height and 0.6 m in diameter. Broadband double-ridged horn antennas, connected to the VNA through the bulkhead connector, were used as transmit and receive antennas. Antennas were aimed away from each other to reduce the direct energy coupling between them. The
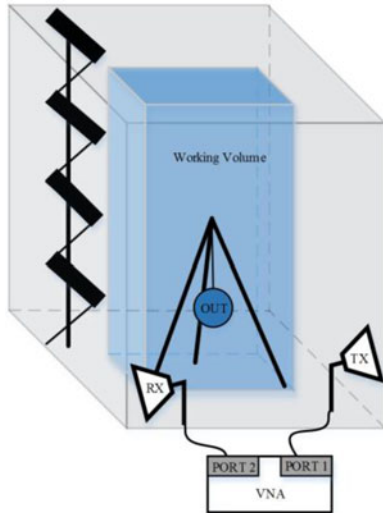
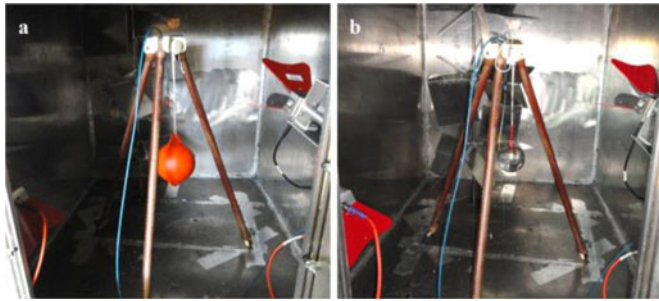Fig. 1. Schematic layout of the reference measurement setup.

Fig. 2. Reverberation chamber interior for the reference measurements: a) water- and HSL-filled large shell and b) water-filled small shell.

schematic layout of the reference measurement setup is shown in Fig. 1.

We used three different objects under test (OUTs) for the reference measurements. The first one was a water-filled sphere in a PVC shell with 15-cm diameter (large shell), the second one was the same 15-cm sphere filled with a broadband head simulating liquid (HSL) [22], and the third was a water-filled sphere in a glass shell with 10-cm diameter (small shell). All OUTs were placed within the chamber's working volume where the average field is expected to have a statistically uniform distribution. The environment inside the reverberation chamber for the reference measurements is shown in Fig. 2.

S-parameters were measured in the frequency range from 1 to 8 GHz. All four scattering parameters were measured (real and imaginary parts). Since the transmitted power into the chamber is assumed to be constant, the received power is proportional to the squared magnitude of S_{21}. The frequency range of interest was measured in 32 001 points with 218.75-kHz sample spacing. During all measurements, the input power was set at 0 dBm. The scattering parameters were measured using a mode-tuned mechanical stirring technique. The results were gathered in steps of 6° of stirrer rotation, which yielded 60 discrete measurement points per one full stirrer turn. The final value of *S*-parameters magnitude was obtained by averaging measured results for all discrete stirrer orientations.
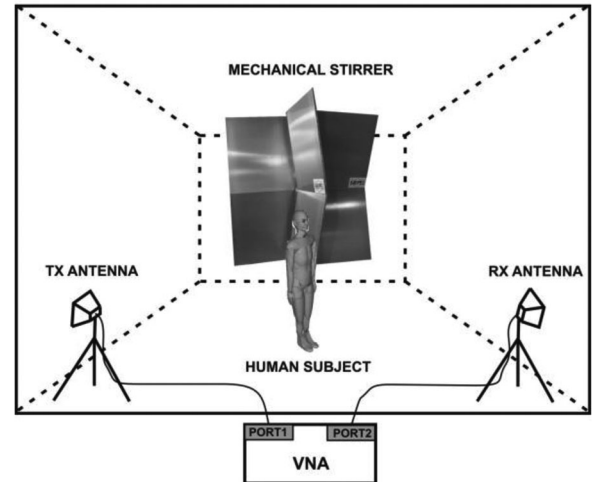

Fig. 3. Schematic layout of the human-body measurement setup.

B. Human-Body and Water Jugs Measurements

The main goal of this contribution was to measure the ACS of an average human body in the upright posture. Considering a human body as the OUT, we needed a reverberation chamber capable of accommodating an average human in the upright posture and still preserving the reverberant behavior; i.e., not being overloaded. Hence, the measurements were performed inside a reverberation chamber with dimensions: (L) 7.78 m × (W) 4.34 m × (H) 3.10 m. This size of the reverberation chamber allows measurements in the frequency range starting from about 120 MHz. The schematic layout of the measurement setup is shown in Fig. 3. The mode stirring was achieved with a single mechanical stirrer made of aluminum panels, mounted between ceiling and floor (see Fig. 4).

Measurements were performed on a real human body and the cylindrical water-filled model shown in Fig. 5, both in an upright posture. The human body was 1.79 m high and weighed 72.5 kg. On the other hand, the cylindrical water-filled model consisted of three 50-cm high jugs. Each jug contained approximately 17 liters of water. The water jugs were stacked one above the other in an upright posture, supported by a PVC structure, as shown in Fig. 5. The complete water model was 1.5 m high and weighed 51 kg. According to [23], the total water content for a human of average weight (70 kilograms) is approximately 50 liters, representing ∼70% of the total body weight. Considering the body water content as the observed parameter, the cylindrical model that was used well describes an average human body.

Another important parameter commonly used to predict the ACS is (body) surface area [17]. Based on the ACS measurements of the cylinder model containing three water-filled jugs and the linear regression of the ACS against the surface area [17], we predicted the ACS of the cylinder model containing four and five water-filled jugs.

The CW signal was generated and monitored by a VNA from 200 MHz to 8 GHz. The desired frequency range was divided into two subranges; one from 200 MHz to 1 GHz, where a pair of log-periodic antennas was used and another from 1 to 8 GHz, where we used a pair of double-ridged horn antennas.
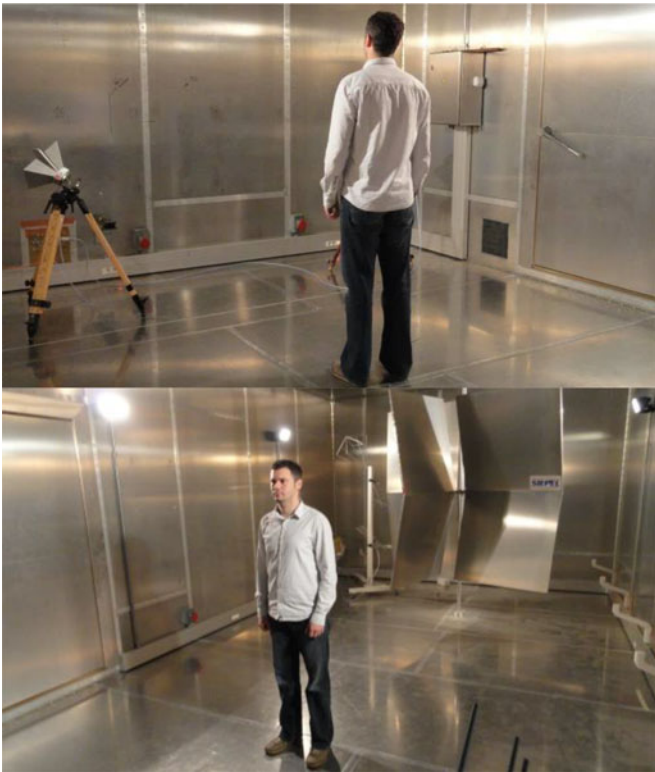
Fig. 4. Reverberation chamber interior for the human-body measurements (front and back view).
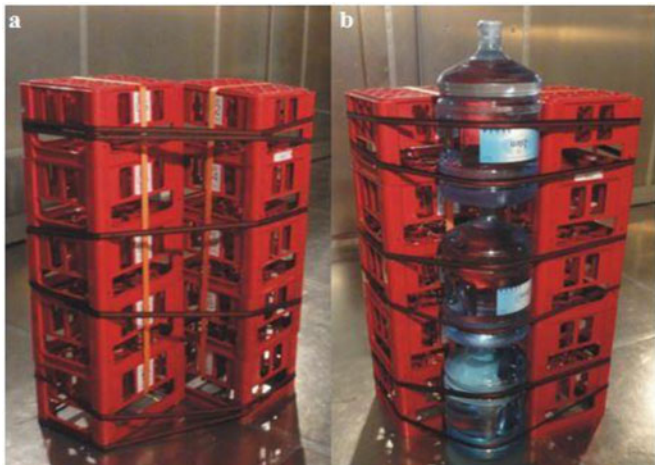

Fig. 5. Reverberation chamber interior for the water jugs measurements: a) Support structure and b) Cylindrical water model with support.

As with the reference measurements, the real and imaginary parts of all four scattering parameters were measured. The frequency range of interest was divided into 39 subranges each having a width of 200 MHz. In each subrange, the *S*-parameters were measured in 801 measurement points with a spacing of 25 kHz, which finally resulted in 31 201 measurement points in the total observed frequency range from 200 MHz to 8 GHz. During all measurements, the input power was set at 0 dBm. The scattering parameters were measured by use of a mode-tuned mechanical stirring technique. The results were gathered in steps
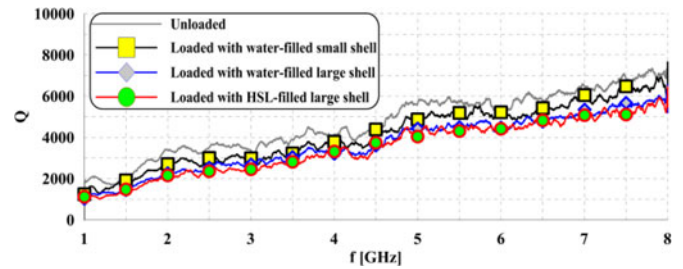

Fig. 6. *Q* factor measurements of unloaded chamber and chamber loaded with reference OUTs.

of 5° of stirrer rotation, which yielded 72 discrete measurement points per one full stirrer turn.

IV. RESULTS

Here, we present the results of the reference OUTs and human-body OUT absorption characteristics given in terms of the ACS and the absorption effectiveness (AE). The ACS can be determined from the measured *Q* factor (i.e., normalized transmission factor *G*) of the unloaded and loaded reverberation chamber, respectively. The AE was given as a difference of the normalized transmission factor measured without and with the OUT placed within the chamber

$$\langle \text{AE} \rangle = 10 \log G_{\text{unloaded}} - 10 \log G_{\text{loaded}}. \quad (8)$$

In this section, we present the validity of the used approach by performing the reference measurements (using spherical OUTs). After that, we proceed with the work that extends the current study by performing the measurements on: 1) the cylindrical water model that can be used as a good substitute (phantom) of the real human and 2) the real human in the upright posture with the hands down. Note that given ACS references mainly study humans in the sitting posture [15], [16]. In [17], three different postures were studied; seated, fetal, and star (standing with hands up) posture. The idea presented here was to measure the posture that was not previously studied.

A. Reference Measurement Results

Placing a lossy OUT inside a reverberation chamber changes its properties which are evident from the *Q* factor alteration. The *Q* factor results of the unloaded chamber and the chamber loaded with three different reference OUTs are shown in Fig. 6. The unloaded chamber *Q* varied with frequency from approximately 2000 at 1 GHz to 7500 at 8 GHz; adding the lossy objects lowered the chamber's *Q*. The obvious difference in chamber's *Q* due to the lossy object presence presents a good motivation for determining the absorption characteristics of the OUTs responsible for *Q* factor alterations. Hence, the interesting parameter pointing out the absorption characteristics of the loading objects presents the AE. Based on *Q* difference between unloaded and loaded chamber, it is possible to determine each OUT's AE, as given in Fig. 7. The OUT that had the highest AE (HSL-filled large shell) had also the largest impact on the chamber's *Q*, and vice versa.
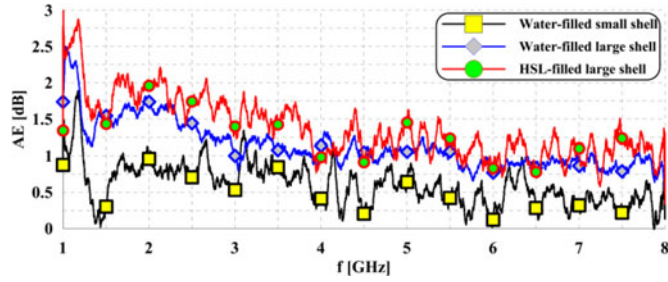
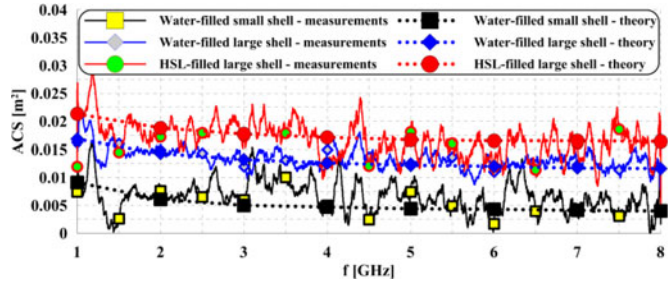Fig. 7.   AE measurements of reference OUTs.

Fig. 8.   Measured and analytically calculated ACS of reference OUTs.

The ACS of three different OUTs was calculated with (7), where normalized transmission factor G was obtained from the measured scattering parameters with (6), averaged over 60 stirrer orientations. The ACS results are given in Fig. 8. Since the HSL-filled large shell presented the highest loading scenario, i.e., had the highest AE, whereas the chamber's Q was the lowest, and its ACS was also expected to be the highest, which measurements confirmed. Similarly, the water-filled small shell had the lowest AE of all tested reference OUTs and therefore had the lowest ACS.

Additionally, the measured ACS was compared to the analytically obtained results. Analytical calculations were based on the Mie scattering theory. A code developed in [24] was used to calculate the theoretical values of the ACS for three different reference OUTs. Good agreement between the measured and theoretical ACS values for all reference OUTs is shown in Fig. 8.

B. Human Model Results

The measurements of the *S*-parameters were performed first for the unloaded chamber (empty chamber or chamber loaded only with the support structure) and then for the loaded chamber (human body or cylindrical water model present). Measurements of the unloaded chamber were used as the reference measurements. Q factors are shown in Fig. 9. Since similar Q results are observed for both the empty chamber and the chamber containing only the support structure, we see that the support structure does not contribute to the chamber's loss, and this case can be considered as the unloaded chamber measurement.

Based on the Q factor difference between the unloaded and loaded chamber, we calculated the AE, shown in Fig. 10, and the ACS, shown in Fig. 11. The results of human body ACS are
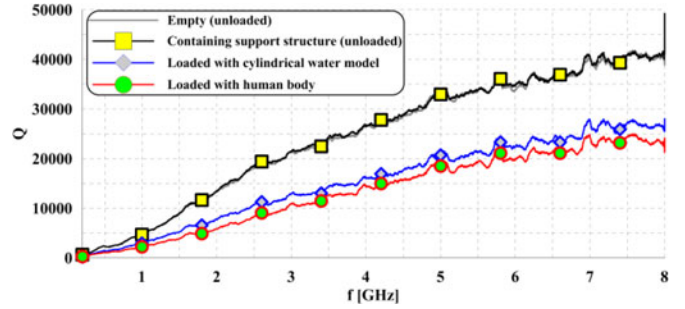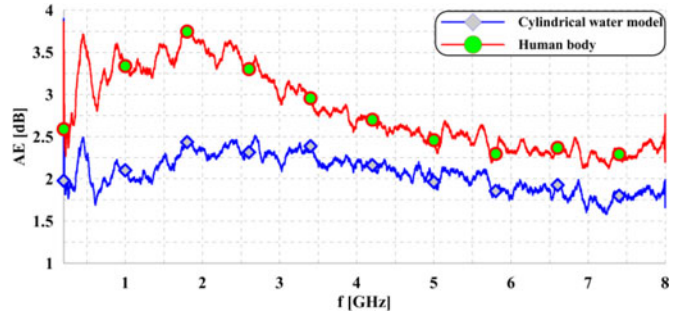

Fig. 9. Q factor measurements of unloaded chamber (empty and containing support structure) and chamber loaded with human body and water jugs.

Fig. 10.   AE measurements of the real human body and water jugs.
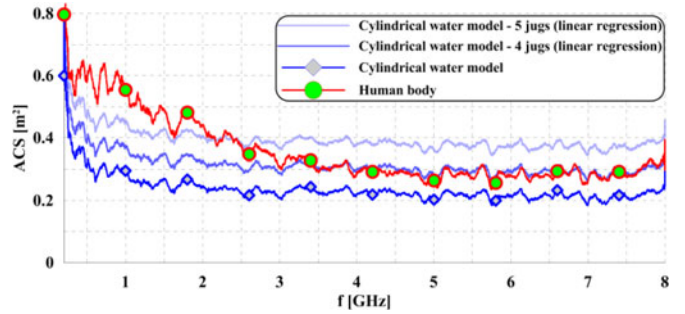
Fig. 11.   ACS measurements of the real human body and water jugs.

in good agreement with the results reported by other groups [2], [15]–[17]. Compared to the real human body, the cylindrical water model, consisted of three water-filled jugs, showed lower values of the AE and ACS especially in the lower frequency range. Since the body water content presents the dominant but not the only absorption contribution, the differences between the calculated ACS of the real human body and the cylindrical water model were expected. Possible better agreement could be achieved by use of the cylindrical model filled with the saline solution [25].

Based on the measured ACS of the cylindrical water model, which consisted of three water jugs, we calculated the ACS of the model containing four and five water-filled jugs, respectively. The approach was based on the linear regression model [17]. In [17], the linear regression of the ACS against the surface area was assumed for the model capable of predicting the ACS. The

ACS results of the linear model containing four and five jugs are also given in Fig. 11. While five jugs overestimate human ACS, best agreement can be observed for four jugs, especially above 3 GHz, which proves that this model can be used to emulate a real human body.

The ACS measurements of the real human body and cylindrical water model took approximately 2 h each and the person needed to stay still during measurements. Even though the ACS discrepancies in a lower frequency range between the cylindrical water model and the real human body exist, they can still be very useful, especially considering how time-consuming measurements such as the proposed ones are.

We measured the maximum ACS of the average human body as approximately 0.6 m^2 at 200 MHz. It fell to approximately 0.3 m^2 at 4 GHz and then slowly rose to approximately 0.35 m^2 at 8 GHz. In the meantime, the water phantom, based on the linear regression model for four water jugs, showed an ACS of approximately 0.5 m^2 at 200 MHz. Above 3 GHz, phantom showed excellent agreement with real human body.

V. CHAMBER VALIDATION AND MEASUREMENT UNCERTAINTY

In order to perform reliable measurements, chamber calibration needs to be performed. The aim of the calibration is to prove the spatial uniformity (SU) within the working volume for all polarizations and given number of stirrer orientations. We performed the calibration for both chambers according to [16]. The data were collected by the receive antenna at eight ($i = 1, 2, \ldots, 8$) different locations that form the corners of the working volume, while the transmit antenna was kept at the fixed location.

The SU was expressed in terms of the standard deviation of the normalized transmission factor G for three different polarizations ($j = 1, 2, 3$) and the total dataset. The total dataset was represented by 24 measurements gathered by combining three individual polarization components at eight measurement locations.

The arithmetic mean of G for each polarization component at each frequency is given by

$$\bar{G} = \frac{\sum\limits_{i=1}^{8} G_i}{8}. \tag{9}$$

Similarly, the total arithmetic mean of G equals

$$\bar{G}_{x,y,z} = \frac{\sum\limits_{i=1}^{8} \sum\limits_{j=1}^{3} G_{i,j}}{24}. \tag{10}$$

The SU is then expressed in terms of the standard deviation given as

$$\sigma = \sqrt{\frac{\sum\limits_{i=1}^{8} \left(G_i - \bar{G}\right)^2}{8 - 1}} \tag{11}$$

$$\sigma_{x,y,z} = \sqrt{\frac{\sum\limits_{i=1}^{8} \sum\limits_{j=1}^{3} \left(G_{i,j} - \bar{G}\right)^2}{24 - 1}} \tag{12}$$

TABLE I
UNCERTAINTY BUDGET

Uncertainty source	SU	VNA	E-Cal
Value	1.4 dB	0.2 dB	0.1 dB
Distribution		Normal	
Divisor		1	
Standard uncertainty	1.4 dB	0.2 dB	0.1 dB
Sensitivity coefficient		1	
Uncertainty	1.4 dB	0.2 dB	0.1 dB
Combined uncertainty		1.42 dB	
Expanded uncertainty		2.84 dB	

where σ is the standard deviation of each polarization component, respectively, and $\sigma_{x,y,z}$ is the standard deviation of the total normalized transmission factor. The standard deviation is expressed in decibels relative to the arithmetic mean as

$$\sigma_{\text{dB}} = 10\log\frac{\sigma + \bar{G}}{\bar{G}}. \tag{13}$$

The standard deviation calculated from (13) for both chambers loaded by the reference OUTs or human models was slightly lower than 1.4 dB. This represented the major contribution to the overall measurement uncertainty. The uncertainty budget, which includes three sources of the uncertainty (SU, VNA drift, and electronic calibration module drift), is given in Table I. The expanded uncertainty obtained for the reverberation-chamber-based ACS measurements was ±2.84 dB. Note that the uncertainty estimation was conservative. The SU was determined in the Cartesian field, even though the ACS actually depends on the total field, which generally has smaller variations. Therefore, true measurement uncertainty should be lower than that given in Table I.

VI. CONCLUSION

In this paper, we presented broadband results for measured human body ACS in a reverberation chamber. Human body ACS is an important parameter for proper assessment of human exposure due to the electromagnetic fields inside highly reflective environments. Before performing the measurements on a real human body, the approach was verified on simple lossy objects, spherically shaped and filled with water and solution simulating an adult human head. Measurements on those canonical OUTs were compared with analytically calculated ACS results and good agreement was achieved.

Additionally, we proposed a simple cylindrical human phantom made of vertically stacked water-filled jugs. The phantom had the same water content as an average human body. The differences in measured ACS between the real human body and the phantom were within the calculated measurement uncertainty. Therefore, the created phantom was a very useful measurement artifact, especially if we consider time-consuming measurements involving humans.

The ACS study will enable us to better estimate the influence of people on a diffuse environment Q, yielding a better understanding of the phenomena related to both, human exposure (dosimetry aspect) and propagation (communication aspect) in such environments.

Future study could include more thorough measurements on a larger sample of subjects in different postures. Based on those results, we believe it would be possible to accurately relate the ACS to the total body surface parameter which could later be used for proper dosimetry and communication studies of human populated highly reflective environments.

REFERENCES

[1] D. Kajfez, *Q Factor*. Oxford, U.K.: Vector Fields, 1994.

[2] G. C. R. Melia, M. P. Robinson, I. D. Flintoft, A. C. Marvin, and J. F. Dawson, "Broadband measurement of absorption cross section of the human body in a reverberation chamber," *IEEE Trans. Electromagn. Compat.*, vol. 55, no. 6, pp. 1043–1050, Dec. 2013.

[3] M. P. Robinson, J. Clegg, and A. C. Marvin, "Radio frequency electromagnetic fields in large conductive enclosures: effects of apertures and human bodies on propagation and field statistics," *IEEE Trans. Electromagn. Compat.*, vol. 48, no. 2, pp. 304–310, May 2006.

[4] T. Nguyen, "RF loading effects of aircraft seats in an electromagnetic reverberating environment," in *Proc. 18th Digital Avionics Syst. Conf.*, Oct. 24–29, 1999, vol. 2, pp. 10.B.5-1–10.B.5-7.

[5] U. Carlberg, P.-S. Kildal, A. Wolfgang, O. Sotoudeh, and C. Orlenius, "Calculated and measured absorption cross sections of lossy objects in reverberation chamber," *IEEE Trans. Electromagn. Compat.*, vol. 46, no. 2, pp. 146–154, May 2004.

[6] A. Gifuni, "On the measurement of the absorption cross section and material reflectivity in a reverberation chamber," *IEEE Trans. Electromagn. Compat.*, vol. 51, no. 4, pp. 1047–1050, Nov. 2009.

[7] *IEEE Standard for Safety Levels with Respect to Human Exposure to Radio Frequency Electromagnetic Fields, 3 kHz to 300 GHz*, IEEE Standard C95.1, 1999.

[8] D. Senic, C. L. Holloway, J. M. Ladbury, G. H. Koepk, and A. Sarolic, "Absorption characteristics and SAR of a lossy sphere inside a reverberation chamber," in *Proc. Int. Symp. Electromagn. Compat.*, 2014, pp. 962–967.

[9] D. Senic, "Human exposure and wireless communication aspects of electromagnetic wave absorption in dissipative objects inside reverberant environments," Ph.D. dissertation, Faculty Elect. Eng., Mech. Eng. Naval Archit., University of Split, Split, Croatia, 2014.

[10] A. Sarolic and D. Senic, "Novel method for practical SAR determination in indoor exposure scenarios without the need for EMF measurements, based on reverberation chamber theory," in *Proc. Bioelectromagn. Soc.*, Jun. 14–19, 2015, pp. 324–328.

[11] A. Bamba, W. Joseph, J. B. Andersen, E. Tanghe, G. Vermeeren, D. Plets, J. O. Nielsen, and L. Martens, "Experimental assessment of specific absorption rate using room electromagnetics," *IEEE Trans. Electromagn. Compat.*, vol. 54, no. 4, pp. 747–757, Aug. 2012.

[12] G. Vermeeren, W. Joseph, C. Olivier, and L. Martens, "Statistical multipath exposure of a human in a realistic electromagnetic environment," *Health Phys.*, vol. 94, no. 4, pp. 345–354, Apr. 2008.

[13] A. Bamba, W. Joseph, E. Tanghe, G. Vermeeren, and L. Martens, "Circuit model for diffuse multipath and electromagnetic absorption prediction in rooms," *IEEE Trans. Antennas Propag.*, vol. 61, no. 6, pp. 3292–3301, Jun. 2013.

[14] D. Senic, A. Sarolic, and Z. M. Joskiewicz, "Preliminary results of human body average absorption cross section measurements in reverberation chamber," in *Proc. Int. Symp. Electromagn. Compat.*, 2013, pp. 887–890.

[15] G. C. R. Melia, I. D. Flintoft, and M. P. Robinson, "Absorption cross-section of the human body in a reverberant environment," in *Proc. Int. Symp. Electromagn. Compat.*, Rome, Italy, Sep. 2012, pp. 1–6.

[16] I. D. Flintoft, G. C. R. Melia, M. P. Robinson, J. F. Dawson, and A. C. Marvin, "Rapid and accurate broadband absorption cross-section measurement of human bodies in a reverberation chamber," *IOP Meas. Sci. Technol.*, vol. 26, no. 6, pp. 065701–1–065701-9, Jun. 2015.

[17] I. D. Flintoft, M. P. Robinson, G. C. R. Melia, J. F. Dawson, and A. C. Marvin, "Average absorption cross-section of the human body measured at 1 -12 GHz in a reverberant environment: Results of a human volunteer study," *IOP Phys. Med. Biol.*, vol. 59, no. 13, pp. 3297–3317, Jul. 2014.

[18] D. A. Hill, *Electromagnetic Fields in Cavities*. Piscataway, NJ, USA: IEEE Press, 2009.

[19] O. Pena and U. Pal, "Scattering of electromagnetic radiation by a multi-layered sphere," *Comput. Phys. Commun.*, vol. 180, pp. 2348–2354, 2009.

[20] *Electromagnetic Compatibility (EMC)—Part 4–21: Testing and Measurements Techniques–Reverberation Chamber Test Methods*, IEC Standard 61000-4-21, May 2005.

[21] J. Ladbury, G. Koepke, and D Camell, "Evaluation of the NASA Langley research center mode-stirred chamber facility," Nat. Inst. Standards Technol., Boulder, CO, USA, Tech. Note 1508, 1999.

[22] *CTIA Broadband Fluid Batch no. CTIA 3.2.*, IndexSAR Ltd., Newdigate, U.K., 2013.

[23] A. C. Guyton, *Textbook of Medical Physiology*. Philadelphia, PA, USA: Elsevier, 2006.

[24] C. Matzler, "MATLAB functions for Mie scattering and absorption," Univ. Bern, Bern, Switzerland, Tech. Rep. 2002-08, 2004.

[25] D. A. Hill, M. T. Ma, A. R. Ondrejka, B. F. Riddle, M. L. Crawford, and R. T. Johnk, "Aperture excitation of electrically large, lossy cavities," *IEEE Trans. Electromagn. Compat.*, vol. 36, no. 3, pp. 169–178, Aug. 1994.

Damir Senic (S'09–M'16) received the M.Sc. and Ph.D. degrees from the Faculty of Electrical Engineering, Mechanical Engineering and Naval Architecture, University of Split, Split, Croatia, in 2008 and 2014, respectively.

He is currently with the Communications Technology Laboratory, National Institute of Standards and Technology, University of Colorado Boulder, Boulder, CO, USA, as a Postdoctoral Research Associate through the Professional Research Experience Program. His research interests include millimeter wave radiocommunications, electromagnetic measurements, electromagnetic compatibility and bioeffects of EM fields.

Dr. Senic received Richard E. Merwin Award of IEEE Computer Society for exemplary involvement in IEEE activities and excellent academic achievement in 2013.

Antonio Šarolić (S'99–M'05) received the Ph.D. degree in electrical engineering from the University of Zagreb, Zagreb, Croatia, in 2004.

He joined the Faculty of Electrical Engineering, Mechanical Engineering and Naval Architecture (FESB), University of Split, Split, Croatia, in 2006, where he is currently a Professor of electrical engineering, Chair of applied electromagnetics, and the Head of Laboratory for EMC and EM research.

He is the proposer and the Chair of the ongoing European COST Action BM1309: "European network for innovative uses of electromagnetic fields (EMFs) in biomedical applications," 2014–2018. He was the Project Leader of a recently completed research project "Measurements in EMC and EM health effects research" funded by Croatian Ministry of Science, and now leads the ongoing project "Measurements in bioelectromagnetics." He led or participated in several other research and development projects related to electromagnetic compatibility and applied electromagnetics and has been involved in several related ongoing or completed EU COST Actions.

He teaches a range of courses at FESB, related to applied electromagnetics, electromagnetic compatibility, antennas, wireless communications, and bioelectromagnetics. In 2008, he was awarded the University Grant from IEEE EMC Society, for developing the EMC course at FESB. He is the Chairman of the Croatian Standardization Technical Committee HZN TO E106 "Electromagnetic fields in human environment," and a member of the committee HZN TO E500 "Electromagnetic compatibility."

Dr. Šarolić is a member of IEEE Electromagnetic Compatibility, Antennas and Propagation, and Engineering in Medicine and Biology societies, Bioelectromagnetics Society and European BioElectromagnetics Association, and has served as the Chair of the IEEE EMC Society—Croatia Chapter for four years.

Zbigniew M. Jóskiewicz received the Master's degree in electronic and telecommunication engineering and the Ph.D. degree in telecommunication engineering, both from the Wroclaw University of Technology (WUT), Wroclaw, Poland, in 1994 and 2002, respectively.

He is currently a Technical Manager in the Electromagnetic Compatibility Laboratory, Wroclaw University of Technology. In years 2008–2012, he was the member of Electronic Department Council of the WUT as well as Istitute of Telekomunications, Teleinformatics and Acoustics Council of the WUT.

Dr. Jóskiewicz is the member of the Steering Committee of the EMC Europe—the International Symposium on Electromagnetic Compatibility and the Program Committee of the National Wrocław EMC Workshops. He is also the Secretary of the University Chapter of SIT (Association of the Telecommunications Engineers) and the EMC Section of Electronic and Telecommunications Section of the Polish Academy of Science.

Christopher L. Holloway (S'86–M'92–SM'04–F'10) received the B.S. degree from the University of Tennessee at Chattanooga, Chattanooga, TN, USA, in 1986, and the M.S. and Ph.D. degrees from the University of Colorado at Boulder, Boulder, CO, USA, in 1988 and 1992, respectively, both in electrical engineering.

During 1992, he was a Research Scientist with Electro Magnetic Applications, Inc., Lakewood, CO, USA. His responsibilities included theoretical analysis and finite-difference time-domain modeling of various electromagnetic problems. From the fall of 1992 to 1994, he was with the National Center for Atmospheric Research (NCAR) in Boulder. While at NCAR his duties included wave propagation modeling, signal processing studies, and radar systems design. From 1994 to 2000, he was with the Institute for Telecommunication Sciences, U.S. Department of Commerce in Boulder, where he was involved in wave propagation studies. Since 2000, he has been with the National Institute of Standards and Technology, Boulder, where he works on electromagnetic theory. He is also on the Graduate Faculty at the University of Colorado at Boulder. His research interests include electromagnetic field theory, wave propagation, guided wave structures, remote sensing, numerical methods, metamaterials, measurement techniques, EMC/EMI issues, and atom-based metrology. He is currently serving as the Associate Editor for the IEEE TRANSACTIONS ON ELECTROMAGNETIC COMPATIBILITY.

Dr. Holloway is a member of URSI Commissions A, B, and E. He is currently serving as Chair for US Commission A of the International Union of Radio Science. He was the Chairman for the Technical Committee on Computational Electromagnetics of the IEEE Electromagnetic Compatibility Society from 2000–2005, served as Co-Chair for the Technical Committee on Nano-Technology and Advanced Materials of the IEEE EMC Society from 2006–2011, and served as an IEEE Distinguished Lecturer for the EMC Society from 2004–2006.